

Supporting Information

Non-powered capillary force-driven stamped approach for directly printing nanomaterials aqueous solution on paper substrate

Langlang Yi,^{†,a} Lei Zhao,^{†,a} Qilu Xue,^a He Cheng,^a Hongyan Shi,^{a,b} Jinkun Fan,^a

Shixuan Cai,^a Guoqian Li,^a Bo Hu,^{*a} Liyu Huang,^{*a} Jie Tian^{*ac}

^aSchool of Life Science and Technology, Xidian University, Xi'an 710126, Shaanxi,
PR China

^bKunpad Communication Pty Ltd, Kunshan 710126, Jiangsu, PR China

^cInstitute of Automation, Chinese Academy of Sciences, Beijing 100190, PR China

1. Characterization of Printing Aqueous Solution

In this work, AgNWs, AgNSs, GO and nanogels aqueous solution are all served as the printing ink. And the TEM images of AgNWs, AgNSs, GO and nanogels are shown in Figure S1.

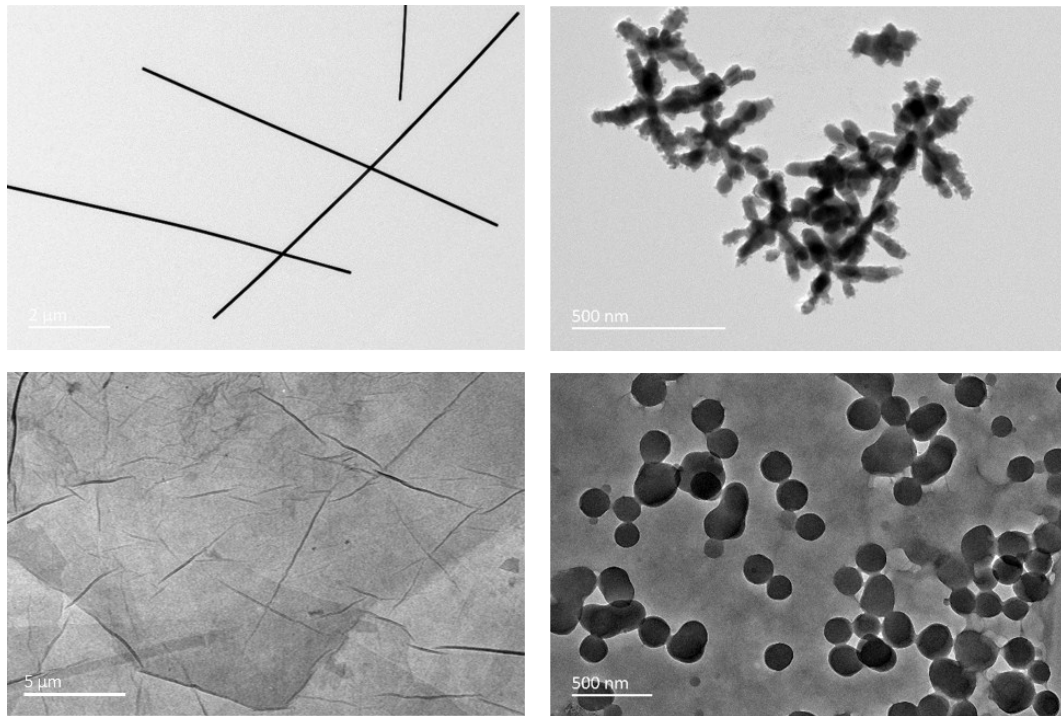


Figure S1. TEM images of AgNWs, AgNSs, GO and nanogels

2. Experimental Parameters of CFDS Approach

In order to provide a relatively comprehensive evaluation of CFDS approach, the experimental parameters are proposed for describing the degree of diffusion, and the uniformity of the resulted patterns. First, several definitions must be clarified. According to the Figure S2, the PD is the ratio between the section area of the capillary channel in 3D-printed stamper and the section area of the designed capillary channel to evaluate the influence of the 3D printing process. The PD should approximate 1, and ‘1’ represents the best performance of 3D printing process. Similarly, the SD is the ratio between the actual area of the stamped pattern and the section area of the designed capillary channel to obtain the theoretical performance. The SD also should approximate 1, and ‘1’ represents the ideal performance of stamping process. Meanwhile, the diffusion rate is the ratio between SD and PD to explore the actual performance of this approach. The diffusion rate should be ≥ 1 , and ‘1’ means no diffusion while ‘ <1 ’ means non-uniformity. Figure S2 presents that the schematic of area region in the CFDS process. Besides, in consideration of that the test pattern is a dot array, the roundness of each dot is calculated to evaluate the fidelity. The roundness equation can be described as:

$$Roundness = \frac{4\pi A}{p^2} \quad (1)$$

where roundness is the value between 0 and 1, A and p represent the area and the perimeter of the closed region, respectively. The roundness is 1 for an actual circle, and the closer the roundness is to 1, the closer it is to an actual circle. Here, the roundness of the 3D-printed capillary channels and the stamping patterns are PP and SP, respectively.

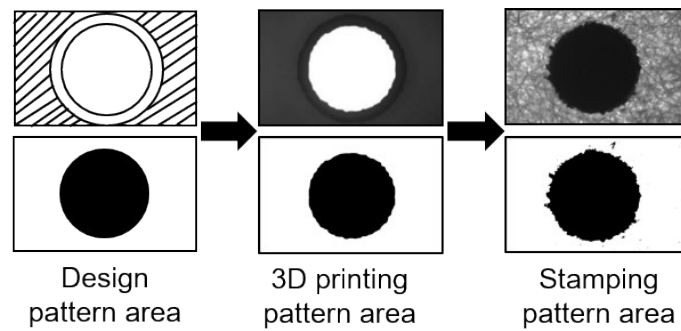
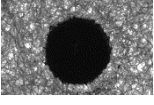

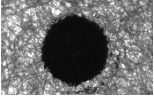
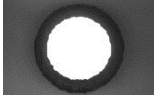
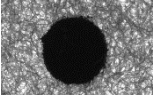
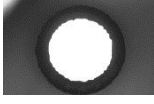
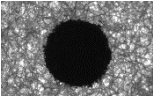
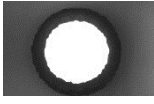
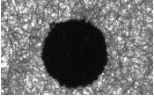
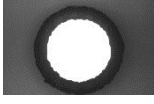
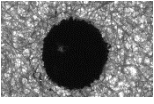
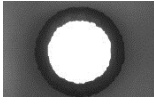
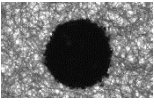
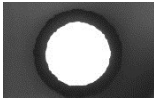
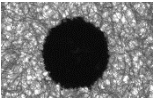
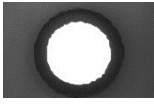
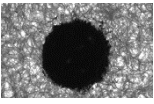
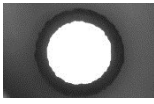


Figure S2. The schematic of area section in the CFDS approach. The size of black section represents corresponding pattern area.

3. Statistics data and analysis process

The section patterns of the designed capillary channel, the section patterns of the capillary channels in 3D-printed stampers and the stamped patterns is analyzed in Figure S2 to indicate the data processing. Then the statistics data and process results of area ratios, roundness and diffusion rates on the paper substrate with the pore size of 20-25 μm are shown in Table S1.

Table S1. Data statistic and analysis process

Design Area (μm^2)	Stamping patterns	Number of black pixel value	PD	PP	Printing patterns	Number of white pixel value	SD	SP	Diffusion rate
1539380		232740	1.08	0.93		208117	0.96	0.88	1.12
		238278	1.10	0.79		209208	0.97	0.88	1.14
		233659	1.08	0.77		207794	0.96	0.87	1.12
		238045	1.10	0.78		209436	0.97	0.87	1.14
		236394	1.09	0.79		210010	0.97	0.87	1.13
		241539	1.12	0.78		206082	0.95	0.87	1.17
		241549	1.12	0.74		212398	0.98	0.88	1.14
		243021	1.13	0.77		209286	0.97	0.87	1.16
		250173	1.16	0.73		212441	0.98	0.88	1.18

*The area of each pixel is $\approx 7.13\mu\text{m}^2$.

4. Idealized theoretical model

According to Figure 1 in the section of process and mechanism of CFDS approach, the approach mainly includes the loading and deposition of nanomaterial aqueous solution.

Essentially, this two processes are manipulated by two dominant equations in capillary flow¹. The equations are as following:

$$h = 2\gamma \cos \theta / \rho g r \quad (2)$$

Here, the γ is the surface tension of the nanomaterial aqueous solution interface, θ is the contact angle of nanomaterial aqueous solution on the 3D printing material, ρ is the density of nanomaterial aqueous solution, g is the gravitational acceleration, and r is radii of the 3D-printed channel.

$$l(t) = \sqrt{\frac{\gamma r \cos \theta}{2\mu} t} \quad (3)$$

This equation is classical model for imbibition of fluid in paper, which is originally derived to interpret one-dimensional capillary flow in a parallel bundle of cylindrical tubes. The l is the distance traveled by the fluid front under capillary pressure, θ is the contact angle of nanomaterial aqueous solution on the filter paper, μ is the nanomaterial aqueous solution viscosity, r is the effective pore radius of paper matrix, and t is the time.

Here, for demonstrating the feasibility of the approach in theory, the processes are ideally simplified by interaction between capillary force and gravitational force. For this idealized model, in the loading process, nanomaterial aqueous solution only experiences the capillary force of 3D-printed channel and gravitational force, and in the deposition process, nanomaterial aqueous solution only experiences the capillary force of paper matrix, gravitational force and the capillary force of 3D-printed channel. As long as the capillary force of 3D-printed channel is stronger than the gravitational force, nanomaterial aqueous solution can be sucked into the channel and complete the loading process. Whereas for the deposition process, the synergistic effect of the capillary force of paper matrix and gravitational force dominate over the capillary force of 3D-printed

channel (F_C) and facilitates the deposition of nanomaterial. Most notably, due to that the paper matrix is equivalent to a parallel bundle of cylindrical tubes, the capillary force of paper matrix approximately equal to the sum of the capillary forces of the paper fiber capillary tubes (F_{CP}) in the paper area covered by the 3D-printed channel. To simply quantify the processes, the capillary forces of all capillary channels is approximated as surface tension of nanomaterial aqueous solution in this idealized theoretical model.

To verify the idealized theoretical model, we have measured the surface tension (Figure S5), contact angle (Figure S6) and viscosity (Figure S7) of water and different nanomaterial aqueous solutions, including AgNWs, AgNSs, GO and Nanogels. According to the model, we have also conducted theoretical calculation and the results are shown in the Table S2. Here, the diameter of 3D-printed channel is 1.4 mm, and the diameters of paper capillary tubes are 20 μm , and the density of water is $1 \times 10^3 \text{ kg/m}^3$. The contrast experiment of water and four nanomaterial aqueous solutions used in the following, including AgNWs, AgNSs, GO and nanogels, as well as theoretical calculation demonstrate that they have approximate capillary force in the 3D-printed channel and the filter paper. Also, the capillary force of 3D-printed channel is stronger than the gravitational force, and synergistic effect of the capillary force of paper capillary tubes and gravitational force is approximately 20 times than the capillary force of 3D-printed channel (Table 1), which perfectly verify the above mechanism. Further contact angle test has demonstrated that different nanomaterial aqueous solutions have similar hydrophilicity as water on the 3D-printed material and filter paper, respectively.

And viscosity test has demonstrated that there is no significant difference between different nanomaterial aqueous solutions and water, and the viscosity of AgNWs aqueous solution varies slowly in the concentration range. This means that the approach is suitable for any nanomaterial aqueous solution. Additionally, a comparison experiment has been conducted to demonstrate the action of ring magnet (Figure S3). The boundary of AgNWs pattern is shown in Figure S4.

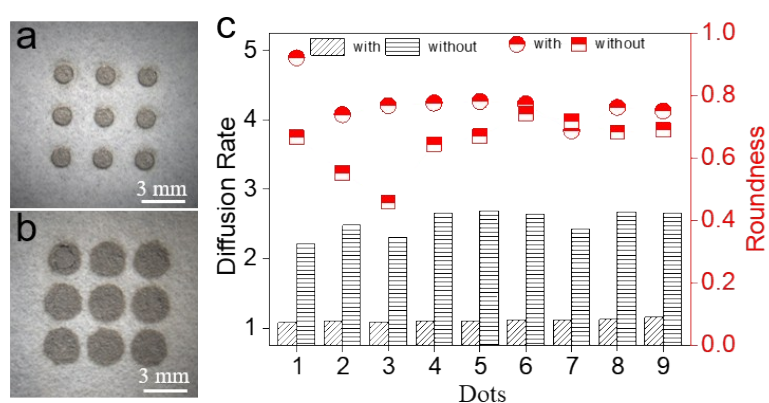


Figure S3. a), b) Optical microscope photos of AgNWs patterned paper substrate with the ring magnet and without it. c) Diffusion rate and roundness of paper substrates with the ring magnet and without it.

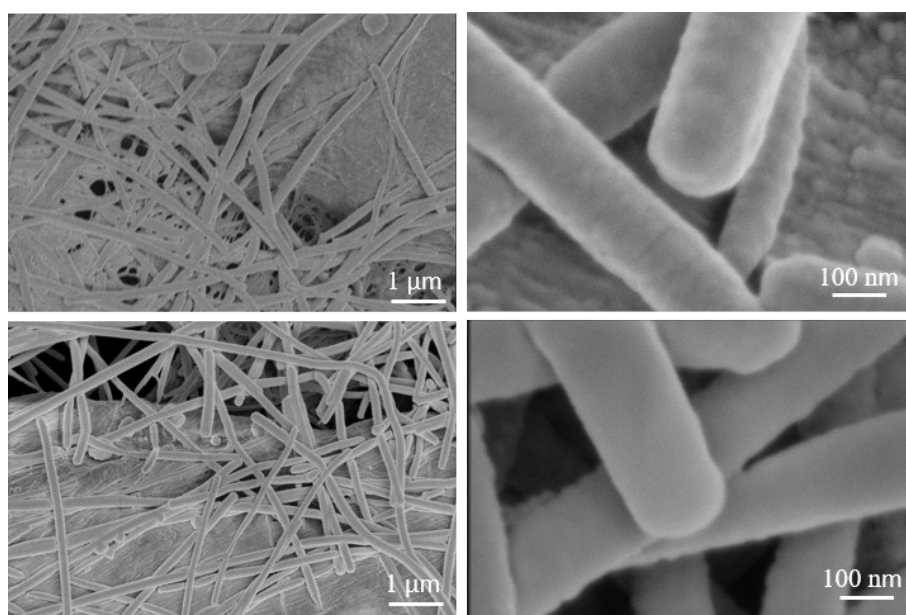


Figure S4. The SEM images of the boundary of AgNWs patterned dot.

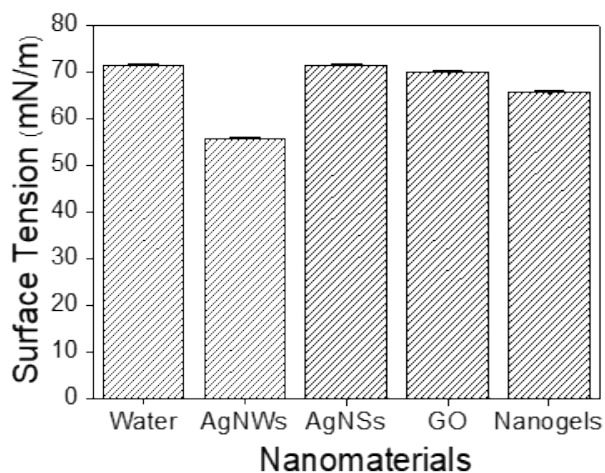


Figure S5. The surface tension of water and different nanomaterial aqueous solutions, including AgNWs, AgNSs, GO and Nanogels. Gravitational Acceleration: $g = 9.8 \text{ m/s}^2$.

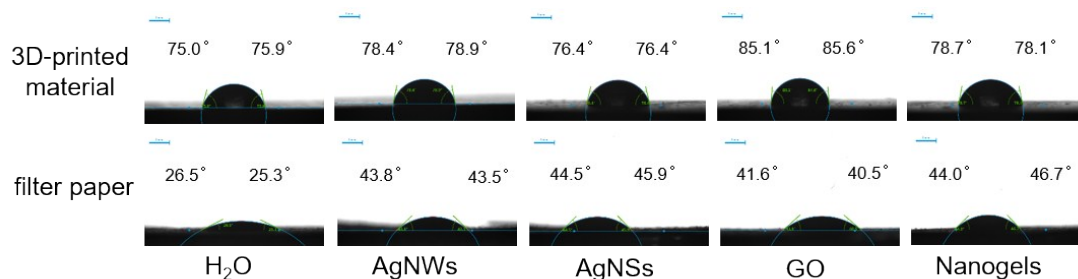


Figure S6. The contact angle of H₂O, AgNWs, AgNSs, GO and Nanogels on the filter paper and on the 3D printing material, respectively.

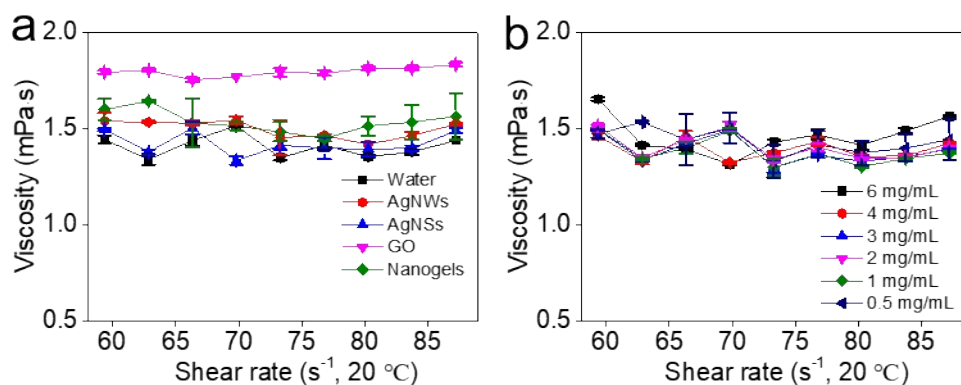


Figure S7. a) The viscosity of water and different nanomaterial aqueous solutions at 20°C, including AgNWs, AgNSs, GO and Nanogels. b) The viscosity of AgNWs with concentration from 0.5 mg/mL to 6 mg/mL at 20°C.

5. Characterization of CFDS Approach

To further characterize the CFDP approach, we have conducted experiments to demonstrate concentration dependence (Figure S8), the diversity of printable substrate (Figure S10), reproducibility (Figure S11), compact degree (Figure S12) of AgNWs patterns, and resolution (Figure S13) of this approach. The data statistics of the blank area of the stamped dots in Figure 2e is shown in Figure S9.

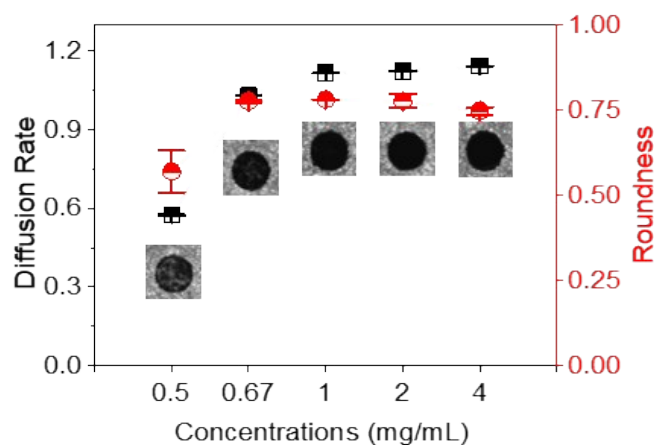


Figure S8. The respective relationship between the concentration and diffusion rate, roundness.

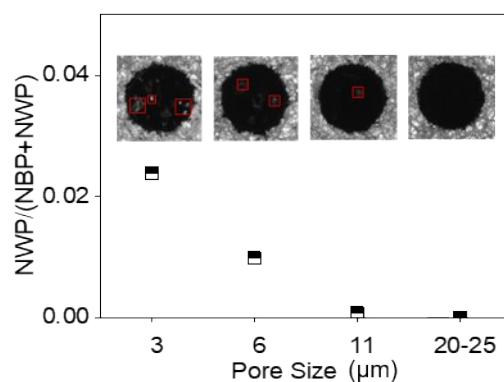


Figure S9. The data statistics of the blank area of the stamped dots in Figure 2e. NBP is the number of black pixel value and NWP is the number of white pixel value in the red frames.

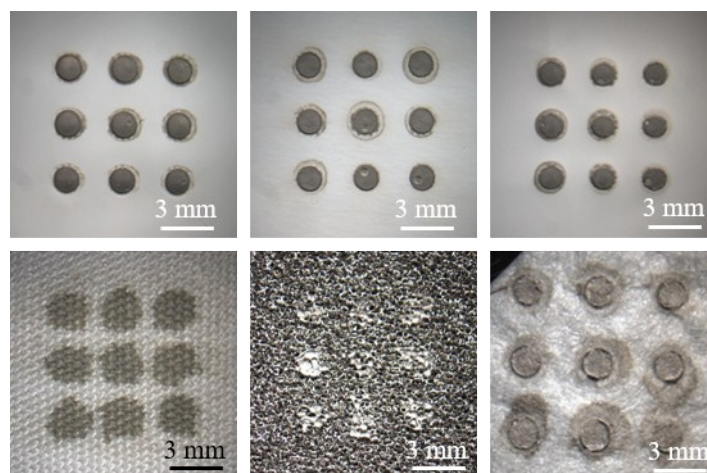


Figure S10. Optical microscope photos of AgNWs patterns on polycarbonate, polyamide, mixed cellulose fiber and polyester, nickel foam and silkworm cocoon porous material, respectively.

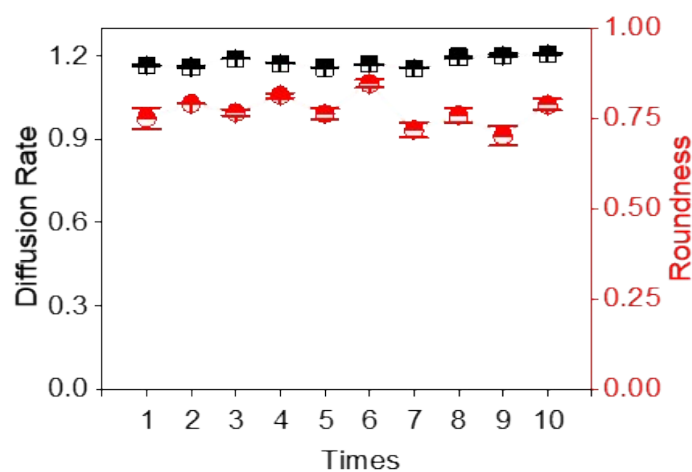


Figure S11. The reproducibility of CFDS approach in the diffusion rates and roundness between 10 repeated trials. The average value of diffusion rate is 1.1776 with RSD of 1.6%, and the average value of roundness is 0.76937 with RSD of 5.5%.

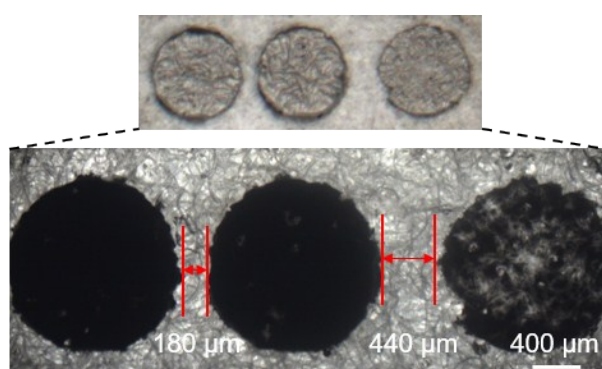


Figure S12. Compact degree of the stamped dots in the CFDS approach. The optical microscopic pictures of stamped AgNWs patterns, where respectively. The minimum space between the stamped dots is 180 μm .

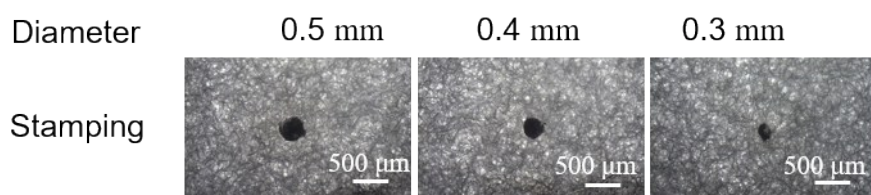


Figure S13. Resolution of CFDS approach. The optical microscopic pictures of stamped AgNWs patterns, where the designed diameters are 0.5 mm, 0.4 mm and 0.3 mm, respectively. The minimum size of the stamped dot is 0.3 mm.

6. Area Ratios and Diffusion Rate of Octagon Patterns

For evaluating printing performance of octagon patterns in detailed, the area ratio and diffusion rate are further studied in Figure S14 and S15, respectively.

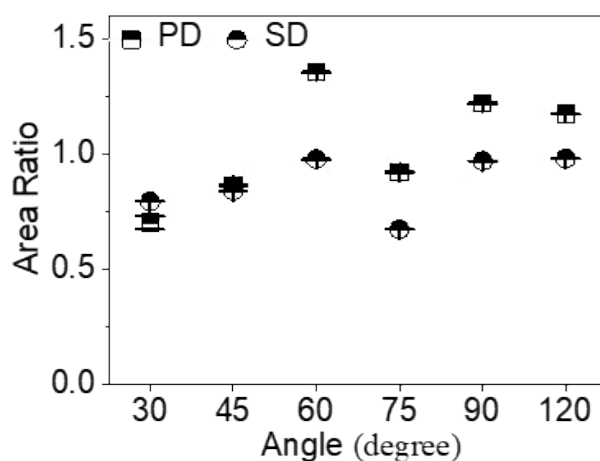


Figure S14. The PD and SD value of octagon patterns.

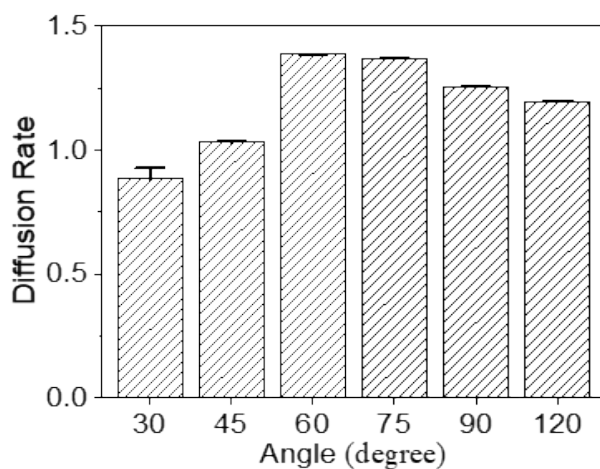


Figure S15. Diffusion rate of octagon patterns.

7. The calculation of AEF

For evaluating the SERS ability of the paper substrate, the analytic enhancement factor (AEF) is calculated by the formula as following: ²

$$AEF = \left(\frac{I_{SERS}}{I_{bare}} \right) \left(\frac{c_{bare}}{c_{SERS}} \right) \quad (4)$$

where I_{SERS} and I_{bare} indicate the integrated peak area of the 4-MBA molecule at 1078 cm^{-1} on the AgNWs patterned paper substrate and the bare paper, respectively. Moreover, c_{SERS} and c_{bare} indicate the concentrations of 4-MBA molecule absorbed on the corresponding substrate, that is, c_{SERS} and c_{bare} are 10^{-7} M and 5×10^{-2} M, respectively.

- 1 M. M. Gong and D. Sinton, *Chem. Rev.*, 2017, **117**, 8447-8480.
- 2 W. Kim, S. H. Lee, J. H. Kim, Y. J. Ahn, Y. H. Kim, J. S. Yu and S. Choi, *ACS Nano*, 2018, **12**, 7100-7108.